International Symposium
On Turbulence and Shear Flow
Phenomena (TSFP-9)
June 30 - July 3, 2015 Melbourne, Australia

NEAR-WALL FEATURES OF VERY LARGE-SCALE MOTIONS IN A TURBULENT CHANNEL FLOW

Jinyul Hwang
Department of Mechanical Engineering
KAIST
Daejeon, Korea
j.yhwang@kaist.ac.kr

Jin Lee
Department of Mechanical Engineering
KAIST
Daejeon, Korea
Lee.Jin@kaist.ac.kr

Hyung Jin Sung
Department of Mechanical Engineering
KAIST
Daejeon, Korea
hjsung@kaist.ac.kr

Tamer A. Zaki
Department of Mechanical Engineering
Johns Hopkins University
Baltimore, Maryland, USA
t.zaki@jhu.edu

ABSTRACT

The spatial and temporal formation of very-large-scale motions (VLSMs) is investigated using data from direct numerical simulation (DNS) of turbulent channel flow at a friction Reynolds number $Re_\tau = 930$. The physical structures of negative and positive streamwise velocity disturbances (u) are examined. The population and area fraction of the structures reveal that negative-u regions are organized into long streamwise extent as compared with positive-u regions whose streamwise length is dominantly less than 3δ in the log layer. The conditional correlations show that the footprint of negative-u structure is relatively narrower but longer than that of positive counterpart. This difference is due to the opposite spanwise motions in the vicinity of their footprints which are the congregative (negative-u) and dispersive (positive-u) motions in the near-wall region induced by the ejection and sweep events associated with the outer large-scale structures. Instantaneous perturbations fields show that near-wall streaks beneath the merging event undergo a spanwise congregative migration. The time series of conditionally-averaged velocity fields demonstrate that this congregative behavior is generated by a roll motion in the outer region, and enhances the magnitude of the near-wall low-speed streaks. This reduces downstream structure convection speed thus promoting the merging process and the formation of VLSMs. The present study confirms that the top-down and bottom-up interactions are the origin of the local difference in convection velocities of outer large-scale structures, and hence their merging into VLSMs.

INTRODUCTION

Large-scale structures contribute significantly to the transfer of momentum and the generation of turbulent kinetic energy in wall-bounded turbulent flows. Very-large-scale motions (VLSMs) have received particular attention since their spectral signature was noted in the premultiplied energy spectra of turbulent pipe flow (Kim and Adrian 1999). Subsequently, experimental and numerical studies (e.g. del Álamo and Jiménez 2003; Guala et al. 2006; Balakumar and Adrian 2007; Hutchins and Marusic 2007a; Monty et al. 2007; Lee and Sung 2011) confirmed their presence in pipe, channel and boundary layer flows, and that they contribute substantially to Reynolds stresses in the outer regions of the mean-flow profile. In addition, the footprint of the VLSMs extends to the near-wall region and thus sustains the large scales nearer to the wall (Hutchins and Marusic 2007a). The presence of large scales in the near-wall region, however, contradicts scaling of the streamwise turbulence intensity using the friction velocity and the viscous length scale (del Álamo and Jiménez 2003; Hoyas and Jiménez 2006; Hutchins and Marusic 2007a), and underscores that VLSMs and near-wall dynamics are interlinked. Moreover, the outer large scales modulate the small-scale energy in the near-wall region (Hutchins and Marusic 2007b; Mathis et al. 2009).

Although the contribution of VLSMs to wall-bounded turbulence can be quantified using some conventional statistical measures, e.g. in terms of their contribution to the Reynolds stresses (Guala et al. 2006; Balakumar and Adrian 2007; Lee and Sung 2011; 2013), their dynamics remain the subject of active research. Kim and Adrian (1999) conjectured that VLSMs are the concatenation of LSMs in the form of hairpin vortex packets. Recently, Lee et al. (2014) examined the spatial and temporal relationship between LSMs and VLSMs statistically, and their results support the notion of concatenation of LSMs to form VLSM. They found that the low-speed streaks with length 1-3δ in the outer region undergo elongation and merging thus forming VLSMs. The merging process is facilitated by the difference in convection speed of these structures depending on the magnitude of their streamwise velocity fluctuations, u. The results by Lee et al. (2014) motivate a detailed analysis of the merging process starting from its precursors through

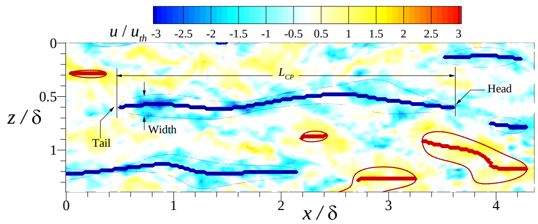

Figure 1. Streamwise velocity fluctuations in the wall-parallel plane at y/δ = 0.15; the thick and thin blue (red) lines represent the $CP = -1$ (CP = +1) and $|\hat{u}| = u_{th}$.

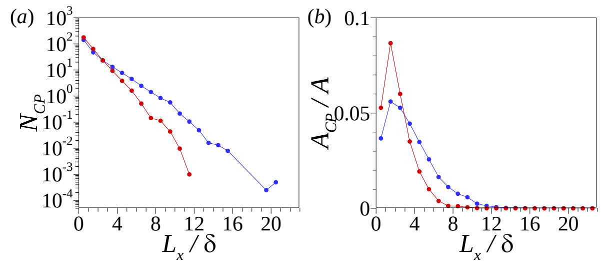

Figure 2. (*a*) Mean number of occurence and (*b*) mean area of the low- (blue) and high-speed (red) streaks at y/δ = 0.15.

its completion and its impact on the near-wall dynamics. The connection between the outer large scales and the near-wall motions was examined by Toh and Itano (2005) in the streamwise minimal channel at Re_τ=349. They reported that the large-scale outer structures are situated between a pair of large-scale circulations, and induce a collective aggregation of low-speed near-wall streaks. In turn, the intense near-wall motions reach up and can potentially have a bottom-up influence on the strength of outer velocity fluctuations.

The objectives of the present study are to characterize the low- and high-speed large-scale structures in turbulent channel flow, and to compare their near-wall footprints. We also examine the role of the associated outer circulation both in terms of the formation of very long negative-u regions and in connection with the near-wall dynamics. To do so, the low- and high-speed structures are compared based on their spatial extent and their spatial characteristics were examined based on the conditional two-point correlations. Empirical observations of the evolution of near-wall and outer structures are reported based on instantaneous flow fields. Using conditional sampling of the flow field around the outer LSMs prior to merging, we examine the interaction between the outer large-scale circulations and the near-wall motions.

NUMERICAL DETAILS

The Navier-Stokes equations for incompressible flow were solved using the fully implicit decoupling method by Kim et al. (2002). The details of the direct numerical simulation (DNS) and the validation are provided in the earlier study by Lee et al. (2014). The streamwise, wall-normal and spanwise directions are denoted x, y and z, respectively, and the associated components of velocity fluctuations are u, v, and w. The superscript + represents quantities normalized by the viscous scales, namely the friction velocity, u_τ, and viscosity, ν. The Reynolds number based on the channel half-height, δ, and the laminar centreline velocity, U_{CL}, is Re_δ = 28,000, and the friction Reynolds number is Re_τ = 930. The domain size in the streamwise and spanwise directions is $(L_x, L_z) = (10\pi\delta, 3\pi\delta)$. A staggered mesh was employed with $4993 \times 401 \times 2497$ grid points in the x, y, and z directions, respectively. The grid sizes in the homogeneous directions are Δx^+=5.86 and Δz^+=3.51. The minimum and maximum wall-normal grid spacings are Δy_{min}^+=0.0287 and Δy_{max}^+=7.31, respectively. The simulation was performed at a constant mass flow rate, and the time step was Δt=0.002U_{CL}/δ, or Δt^+=0.0618, and the averaging period spanned 220 time units. A total of 2,010 snapshots were stored, with each two consecutive fields separated by 0.1 time units.

To investigate the long-u regions in time and space, streak detection techniques are adopted in order to identify the specific motions of interest in the instantaneous fields (Nolan and Zaki 2013; Lee et al. 2014). The threshold $u_{th,raw}$=0.1U_b, where U_b is the bulk velocity (Dennis and Nickels 2011; Baltzer et al. 2013). The detection procedure starts with two spatial filters: a Gaussian filter in the cross-stream plane and a long-wavelength-pass filter (>1δ) in the streamwise direction. Due to the weakened magnitude of u by the filters, the velocity-threshold for filtered flow field ($\hat{u}$) is corrected, $u_{th}(y) = f(y)u_{th,raw}$, where $f(y)$ is the ratio of the correlation functions between u and $\hat{u}$. Neighboring extrema in the spanwise direction thus mark the cores of the velocity disturbances and can be regarded as characteristic projections (CP) of u-structures. Hence, CP=+1 marks high-speed structures and CP=−1 identifies low-speed ones. Figure 1 shows a top view of the u contours at y/δ=0.15. The streamwise length, L_{CP}, of each streak was measured along the line of CP=±1.

LONG STREAKS OF STREAMWISE VELOCITY FLUCTUATIONS

Figure 2(*a*) shows the mean number of occurrence of the negative- and positive-u regions according to their streamwise length, L_{CP}, at y/δ=0.15. The frequencies of occurrence N_{CP} for the negative- (blue) and positive-u (red) regions binned by their streamwise length is displayed in figure 2(*a*). The negative-u region was found up to 20δ but the positive one was detected up to 12δ. Very long feature of negative-u regions observed at y/δ=0.15 represents the length scales of VLSMs which are typically O(10–20δ) in channel and pipe flows (Kim and Adrian 1999; del Álamo et al. 2004; Hoyas and Jiménez 2006; Monty et al. 2007, Lee and Sung 2013). Although the distributions of both negative- and positive-u regions logarithmically decrease according to their length, the negative-u regions tend to be longer than their positive counterparts and the latter is more weighted towards the shorter length. Around 3δ, in particular, the

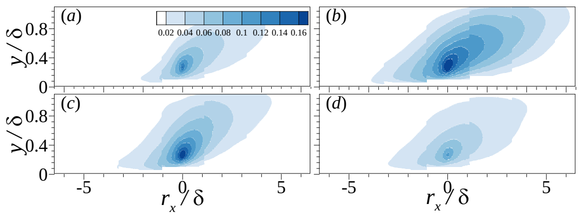

Figure 3. Conditional correlations ($R[u_I, u]$) in the x–y plane (r_z/δ = 0). (*a*) nLSM (I=1); (*b*) nVLSM (I=2); (*c*) pLSM (I=3); (*d*) pVLSM (I=4).

frequencies of low- and high-speed start to appear significant difference as the streamwise length increase. It indicates that the low-speed regions are more organized in the streamwise direction and exist relatively longer structure than the positive counterparts in each instantaneous flow field.

To analyze the spatial extent occupied by negative- and positive-u structures, figure 2(*b*) shows the area fraction of the streaks within each length bin in the y/δ=0.15 surface. The area with the specified length bin was normalized by the total area of the wall-parallel plane ($A = L_x \times L_z$). Although the shorter structures of negative- and positive-u occur more frequently in figure 2(*a*), the area fraction has a peak between 1δ and 3δ in length. The area occupied by 1-3δ streaks, nominally considered as the length scale of LSMs (Adrian et al. 2000; Guala et al. 2006; Balakumar and Adrian 2007), is dominant per instantaneous field. In addition, the area fraction of positive-u crosses the negative counterparts around L_{CP}=3δ similar to the trend of frequencies observed in figure 2(*a*). Due to low frequencies of positive-u regions (>3δ) the area fraction of them rapidly drops as compared with the negative-u structures. Moreover, the area fraction of negative-u regions with length longer than 3δ possess 15% (14% for L_{CP}<3δ) as compared with that of positive counter parts, 7% (20% for L_{CP}<3δ).

The VLSMs are originally defined as motions with streamwise Fourier wavelengths greater than 3δ in Guala et al. (2006). Several study used this length criteria to differentiate LSMs and VLSMs. In physical space, Baltzer et al. (2013) defined the VLSMs longer than 3δ at y/δ=0.15 surface and the contribution to the Reynolds shear stress of these motions were computed at this wall-normal position (Lee and Sung 2011; 2013). In addition, Lee et al. (2014) computed the JPDF of the streamwise length of CP and the number of long (>1δ) characteristic spines, which fairly well represent the characteristics of LSMs, to examine spatial association of LSMs in a VLSM. They showed that L_{CP} longer than 2.9δ contains more than 2 of LSMs. This is close to the previous critical length 3δ (Guala et al. 2006; Balakumar and Adrian 2007; Dennis and Nickels 2011; Baltzer et al. 2013). In the present study, hence, streamwise-extended regions of contiguous CP at y/δ=0.15 were classified into LSM and VLSM based on 3δ and these motions were categorized according to their sign (negative, ``n'', and positive, ``p''). This classification yields the

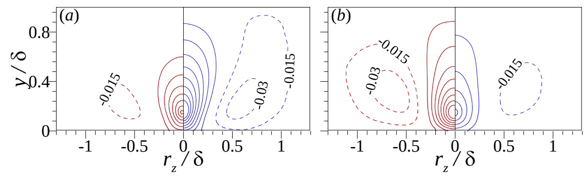

Figure 4. Conditional correlations ($R[u_I, u]$) in the y–z plane (r_x/δ = 0). (*a*) nLSM (left; I=1) and nVLSM (right; I=2); (*b*) pLSM (left; I=3) and pVLSM (right; I=4).

following four categories: nLSM (1δ<$L_{CP}|_{CP=-1}$<3δ; hearafter I=1); pLSM (1δ<$L_{CP}|_{CP=+1}$<3δ; I=2); nVLSM ($L_{CP}|_{CP=-1}$>3δ; I=3); pVLSM ($L_{CP}|_{CP=+1}$>3δ; I=4).

CONDITIONAL VELOCITY CORRELATIONS

The spatial characteristics of long-u streaks (nLSM, nVLSM, pLSM, and pVLSM) and their spatial relationship with the velocity fluctuating components are explored by computing conditional two-point correlations. The correlation coefficient (R) is defined as

$$R[u_I, u_j](\boldsymbol{r}) = \frac{\left\langle u_I(\boldsymbol{x}) u_j(\boldsymbol{x}+\boldsymbol{r}) \right\rangle\Big|_{I=n}}{\sigma_u(y_{ref})\sigma_j(y)}, \qquad (1)$$

where the subscripts j represent different components of fluctuating velocity (u,v,w) and σ_j is the standard deviation of j component. From now on, we will refer to the correlation coefficient as correlation.

The streamwise sections (r_z/δ=0) of the correlations are plotted in figure 3. Despite of the different conditions, all contours have a ramp-like shape of the positive correlations which is the general feature of unconditional two-point correlations in the log layer (Hutchins and Marusic 2007a; Baltzer et al. 2013; Sillero et al. 2014). However, the magnitudes and patterns of the correlations are distinct depend on their conditions. The maximum correlation values for nLSM and nVLSM are 0.15 and 0.22, respectively. This suggests a dominance of the streamwise turbulent intensity carried by the VLSMs at this wall-normal location although the population of nVLSMs is less prominent than nLSMs as shown in figure 2(*a*). The correlation of LSMs is inclined with large angle in the streamwise direction compared to the VLSMs with relatively less extend in the streamwise direction. The ramp-like character of the correlations indicates that nLSMs and nVLSMs at y/δ=0.15 are correlated with the streamwise fluctuations in the near-wall region. Both correlations are attached to the wall as a footprint (Hutchins and Marusic 2007a), in particular, the footprint of nVLSMs is obvious than that of nLSMs.

The conditional correlations of pLSM and pVLSM are illustrated in figures 3(*c*,*d*). The correlations of positive-u structures are also inclined to the wall and elongated in the streamwise direction similar with the negative-u structures. However, the maximum correlation values are 0.2 and 0.11 and the streamwise length scales of correlation are 7δ and 6δ, respectively, illustrating that the features are opposite to the

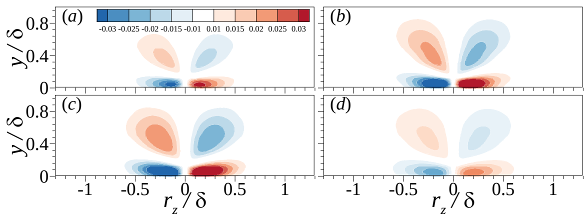

Figure 5. Conditional correlations ($R[u_I, w]$) in the *y*–*z* plane (r_x/δ = 0). (*a*) nLSM (*I*=1); (*b*) nVLSM (*I*=2); (*c*) pLSM (*I*=3); (*d*) pVLSM (*I*=4).

negative counterparts. The pLSMs carry almost two times higher *u* intensity than pVLSM suggesting that they are representative organized motions of positive-*u* in the log layer. This result is consistent with the dominant area fraction of pLSM (20%) than pVLSM (7%) at y/δ=0.15 (figure 2*b*).

Figure 4(*a*,*b*) displays the spatial organization of the correlations in the cross-flow plane (r_x/δ=0). Note that the correlations are shown side-by-side in each panel with LSMs on the left (red) and VLSMs on the right (blue) due to their symmetry in the spanwise direction. The positive values of correlations are varied from 0.02 to 0.16 with an increment of 0.02 and the negative value of them is labelled in each plot. A noteworthy feature is a comparable size of the correlation width between nLSM and nVLSM as compared with their discrepancy of the length scale in the streamwise direction. Based on the spectral filtering, the similarity between the azimuthal scale of the LSM and VLSM was reported that if the VLSMs are created by the streamwise concatenation of LSMs (Kim and Adrian 1999), only the LSMs in the outer layer (y/R>0.5) align to form the VLSMs (Bailey and Smits 2010). The present conditional correlations based on the physical length of motions represent that the small disparity between the spanwise scales of LSMs and VLSMs, even at the same wall-normal position (y/δ=0.15), could support the hypothesis conjectured by Kim and Adrian (1999).

The conditional correlations of pLSM and pVLSM are illustrated in figures 4(*b*). The contours of pLSM correlation reaches up to the core region similar with the nVLSM, revealing that the pLSM is much more dominant motion than the pVLSM. Compared to negative-*u* correlations (figure 4*a*), the patterns of the positive-u cases (figure 4*b*) differ appreciably along the wall-normal direction. The correlations of positive-*u* structures remain their width along the wall-normal direction but the width of negative counterparts gradually decrease close to the wall. In other words, the footprint of positive-*u* structure is wider than negative-*u* one which suggests the near-wall region affected by the outer large-scales is relatively extensive for positive-*u* motions.

To investigate the different footprint shape of *u*-structures observed in figure 4(*a*,*b*), the cross-correlations between the specific *u* events with spanwise fluctuations (*w*), $R[u_I, w]$, were examined in the cross-stream plane. Figure 5 illustrates the cross-correlations ($R[u_I, w]$) at r_x/δ=0. The

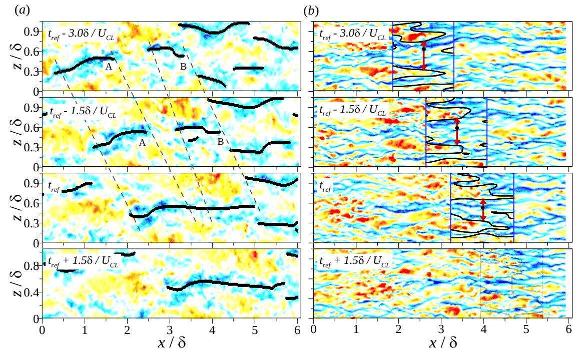

Figure 6. Time sequence of instantaneous flow fields in *x*–*z* plane: (*a*) y/δ = 0.15, (*b*) y^+ = 14.5.

most obvious feature of these correlations is that the higher correlations values appear under the reference position. The peak values are located at (y^+=42, r_z/δ=±0.13); the negative peak on the left and the positive peak on the right. These strong correlations penetrate into the near-wall region, indicating the possibility of the amplitude modulation effect of outer large-scales on the near-wall spanwise fluctuations (Talluru et al. 2013). However, the magnitude of correlations and the direction of the spanwise velocity fluctuations are distinct based on the conditions. The sign of the correlation value represents the dominant direction of spanwise velocity fluctuations. Hence, the negative values on the left and the positive values on the right for negative-*u* conditions (figure 5*a*,*b*) indicate the congregative motions and those for positive-*u* conditions (figure 5*c*,*d*) represent the dispersive motions in the near-wall region. The contours of $R[u_I, u]$ for negative-*u* are gradually narrower under the reference position where as those for positive-*u* are relatively wider in figure 4. This different shape of footprint can be explained due to the opposite direction of spanwise motions in the vicinity of footprint; the congregative/dispersive motions for negative and positive-*u* footprints. The maximum correlation values for nLSM and nVLSM are 0.034 and 0.048, respectively suggesting that the strong congregative motions under the nVLSM. In common with the positive-*u* $R[u_I, u]$, the pLSM has the greater maximum value (0.05) than the pVLSM (0.025) due to extremely low population and area fraction of pVLSM (figure 2). Hence, the nVLSM and pLSM are dominant motions which induce the strong spanwise motions, congregative and dispersive motions, in the near-wall region. In the next section, this spanwise motions are examined during the formation of nVLSM via the merging of streamwise-aligned *u*-regions in the log layer.

FORMATION OF VERY-LARGE-SCALE MOTIONS

Lee and Sung (2011) and Lee et al. (2014) reported that the different convection velocities of upstream and downstream structures lead to this merging process thus creating nVLSMs. This merging is a frequently-observed event based on an assessment of the convection velocities of streamwise aligned structures. The origin of this trend

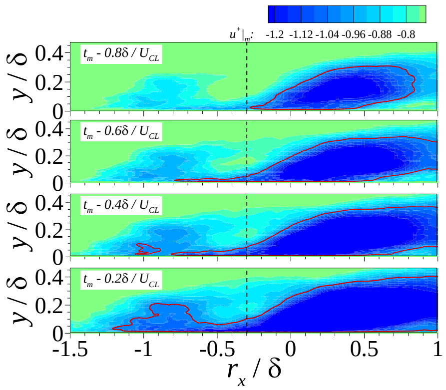

Figure 7. Time sequence of the conditionally-averaged velocity fields, $u^+|_\mathrm{m}$, in x–y plane (r_z/δ = 0).

remains unclear and, in light of the correlation between the events in the outer and near-wall flow, a simultaneous investigation of the two regions during the merging process is required. A time-series of the velocity perturbation field is shown in figure 6, and captures the merging of two streamwise-aligned LSMs at y/δ=0.15. The black lines in figure 6(a) mark the CP in the wall-parallel plane, and represent continuous regions of negative-u. At t_{ref}−1.5δ/U_{CL}, there are two distinct LSMs which are not connected to each other; they are separated by a region of positive velocity perturbation. The streamwise lengths of the upstream and downstream LSMs are on the order of 1-2δ. The upstream LSM moving faster than downstream one. The latter is continuously stretched due to the slower advection velocity of its tail relative to its head. They ultimately merge into a single long streak whose streamwise extent is longer than 3δ. The evolution of the near-wall perturbation field during the outer merging process is illustrated in figure 6(b). The black dot identifies the tail position of the LSM B, and the solid black isocontour marks $\hat{u}=0$. In the marked region, several streaky structures of negative-u are distributed in the span, separated by a weak perturbation field. As the outer LSMs approach one another in the merging process, the near-wall structures congregate within a narrowing window and will ultimately form a wide high-amplitude near-wall structure beneath the outer merging process.

The conditionally-averaged fields are examined in order to provide a statistical account of the merging process and the formation of nVLSMs observed in the time-series from the DNS. The conditionally-averaged perturbation field is defined as

$$\boldsymbol{u}\big|_m(\Delta\boldsymbol{x},\Delta t)=\left\langle u^+ \middle| CP^{DT}\right\rangle\left(\boldsymbol{x}_{ref}-\Delta\boldsymbol{x},t_{ref}-\Delta t\right), \qquad (2)$$

where the superscript DT refers to the reference point being the tail position of the downstream structure, and the reference position for the conditional averaging is y/δ = 0.15. Time was measured relative to a reference time, t_{ref}, where merging takes place. A time sequence of conditionally-averaged velocity fields, $u^+|_m$, is shown in figure 7. Although the reference location for the conditional average is at the tail of an outer large-scale motion, another velocity structure on the order of 1δ in length is predicted upstream of the reference position. At early times, the two outer structures are separated, but their separation decreases in time up to the merging event. The solid contour marks a relatively strong negative-u region which is initially restricted to the downstream structure but is gradually enlarged to include the upstream structure. As time evolves, the isocontour line extends in the upstream direction although the velocity structure convects downstream. This trend reflects the retardation of the tail of the downstream structure prior to merging.

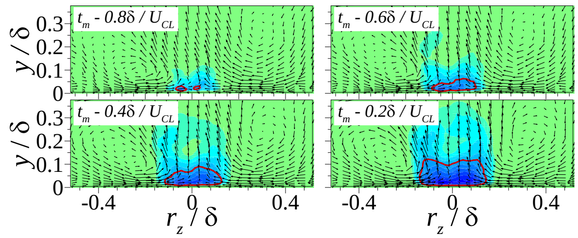

Figure 8. Time sequence of the conditionally-averaged velocity fields, $u^+|_m$, in y–z plane (r_x/δ = –0.3).

Figure 8 shows the time-evolution of the near-wall disturbances in the y–z plane. The vectors are the conditionally-averaged in-plane velocities, and the contours show the streamwise velocity perturbation. In figure 8, the reference location for conditional averaging is r_x/δ=−0.3, which is marked by vertical dashed lines in figures 7. This position is the most upstream end of the strong negative disturbance ($u^+|_m$=−1.0) associated with the downstream structure at t_{ref}−0.8δ/U_{CL}. At early time, the wall-normal extent of the lowest contour level, $u^+|_m$=−0.8, is confined within y/δ<0.1. Moreover, there is a pair of large-scale circulations without a strong low-speed event between them. As time evolves, the flow response to the large-scale vortices is observed in the form of an amplifying negative-u perturbation. There is a rapid growth and intensification of the negative-u field via the congregative motion of near-wall streaks swept by large-scale circulation. In terms of the wall-normal extent, the solid contour initially reaches up to y/δ=0.032 (y^+=30). It subsequently expands and extends beyond y/δ=0.3. Thus, the intense near-wall congregative motion induced by the outer large-scale circulation transforms into a strong streamwise velocity fluctuations at the tail of downstream structure. Because the local convection speed is proportional to the streamwise velocity fluctuations Lee et al. (2014), the intense near-wall motions reduce the convection velocity of the downstream large-scale structure and, ultimately, lead to the merging event with the upstream structure.

SUMMARY AND CONCLUSIONS

The spatio-temporal formation of VLSMs and the accompanying near-wall behavior were investigated by analyzing flow fields from DNS of turbulent channel flow at a friction Reynolds number Re_τ=930. Although the negative-and positive-*u* regions occupy similar area fractions within the disturbance field, they differ when divided into LSM (1-3δ) and VLSM (>3δ). In the log layer, the pLSM occupies a larger area fraction than the negative counterpart. However, the nVLSMs are more frequent than the positive ones. The area fractions are consistent with positive perturbations being generally shorter and wider than negative-*u* structures. Based on the conditional two-point correlation, both the positive and negative-*u* structures penetrate into the near-wall regions as footprint. However, the footprint associated with positive-*u* are relatively wider than their negative counterpart. The different spanwise scale is due to the character of the near-wall motion associated with the large-scale structures: The large-scale circulation associated with sweeps generates diverging wall jets in the spanwise direction, while the large-scale circulation associated with negative-*u* has the form of ejections with near-wall opposing jets. From the time evolution of instantaneous fields, we examined the merging of LSMs to form very-large-scale structures. Beneath the merging event, we demonstrated the presence of a congregative motion in the near-wall region which causes the negative-*u* perturbations to intensify as adjacent streaks aggregate. The width of the resulting near-wall negative-*u* perturbation exceeds the characteristic spanwise scale of near-wall streaks. The dynamics of this process were examined using conditional averages with the reference event being the merging of LSMs at y/δ=0.15. The conditional average confirmed that the intense near-wall regions are a robust feature during the merging process. In other words, the formation of negative VLSMs is strongly related with the congregative near-wall behavior.

ACKNOWLEDGEMENTS

This work was supported by the Creative Research Initiatives (No. 2015-001828) program of the National Research Foundation of Korea (MSIP) and was partially supported by KISTI under the Strategic Supercomputing Support Program.

REFERENCES

Adrian, R. J., Meinhart, C. D., and Tomkins, C. D., 2000, “Vortex organization in the outer region of the turbulent boundary layer”, *J. Fluid Mech.*, Vol. 422, pp. 1-54.

del Álamo, J. C., and Jiménez, J., 2003, “Spectra of the very large anisotropic scales in turbulent channels”, *Phys. Fluids*, Vol. 15(6), L41.

Bailey, S. C., and Smits, A. J., 2010, “Experimental investigation of the structure of large-and very-large-scale motions in turbulent pipe flow”, *J. Fluid Mech.*, Vol. 651, pp. 339-356.

Balakumar, B. J., and Adrian, R. J., 2007, “Large-and very-large-scale motions in channel and boundary-layer flows”, *Phil. Trans. R. Soc. A*, Vol. 365(1852), pp. 665-681.

Baltzer, J. R., Adrian, R. J., and Wu, X., 2013, “Structural organization of large and very large scales in turbulent pipe flow simulation”, *J. Fluid Mech.*, Vol. 720, pp. 236-279.

Dennis, D. J., and Nickels, T. B., 2011, “Experimental measurement of large-scale three-dimensional structures in a turbulent boundary layer. Part 2. Long structures”, *J. Fluid Mech.*, Vol. 673, pp. 218-244.

Guala, M., Hommema, S. E., and Adrian, R. J., 2006, “Large-scale and very-large-scale motions in turbulent pipe flow”, *J. Fluid Mech.*, Vol. 554, pp. 521-542.

Hoyas, S., and Jiménez, J., 2006, “Scaling of the velocity fluctuations in turbulent channels up to Re_τ = 2003”, *Physics of Fluids*, Vol. 18(1), 011702.

Hutchins, N., and Marusic, I., 2007a, “Evidence of very long meandering features in the logarithmic region of turbulent boundary layers”, *J. Fluid Mech.*, Vol. 579, pp. 1-28.

Hutchins, N., and Marusic, I., 2007b, “Large-scale influences in near-wall turbulence”, *Phil. Trans. R. Soc. A*, Vol. 365(1852), pp. 647-664.

Kim, K. C., and Adrian, R. J., 1999, “Very large-scale motion in the outer layer”, *Phys. Fluids*, Vol. 11(2), pp. 417-422.

Kim, K., Baek, S. J., and Sung, H. J., 2002, “An implicit velocity decoupling procedure for the incompressible Navier–Stokes equations”, *Intl J. Numer. Meth. Fluids*, Vol. 38(2), pp.125-138

Lee, J., Lee, J. H., Choi, J.-I., and Sung, H. J., 2014, “Spatial organization of large-and very-large-scale motions in a turbulent channel flow”, *J. Fluid Mech.*, Vol. 749, pp.818-840.

Lee, J. H., and Sung, H. J., 2013, “Comparison of very-large-scale motions of turbulent pipe and boundary layer simulations”, *Phys. Fluids*, Vol. 25(4), 045103.

Mathis, R., Hutchins, N., and Marusic, I., 2009, “Large-scale amplitude modulation of the small-scale structures in turbulent boundary layers”, *J. Fluid Mech.*, Vol. 628, pp. 311-337.

Monty, J. P., Stewart, J. A., Williams, R. C., and Chong, M. S., 2007, “Large-scale features in turbulent pipe and channel flows”, *J. Fluid Mech.*, Vol. 589, pp. 147-156.

Nolan, K. P., and Zaki, T. A., 2013, “Conditional sampling of transitional boundary layers in pressure gradients”, *J. Fluid Mech.*, Vol. 728, pp. 306-339.

Sillero, J. A., Jiménez, J., and Moser, R. D., 2014, “Two-point statistics for turbulent boundary layers and channels at Reynolds numbers up to $\delta^+ \approx$ 2000”, *Phys. Fluids*, Vol. 26(10), 105109.

Talluru, K. M., Baidya, R., Hutchins, N., and Marusic, I. 2014, “Amplitude modulation of all three velocity components in turbulent boundary layers”, *J. Fluid Mech.*, Vol. 746, R1.

Toh, S., and Itano, T., 2005, “Interaction between a large-scale structure and near-wall structures in channel flow”, *J. Fluid Mech.*, Vol. 524, pp. 249-262.